Control of a Fuel-Cell Powered DC Electric Vehicle Motor

Federico Zenith
Sigurd Skogestad
Department of Chemical Engineering
Norwegian University of Science and Technology (NTNU)
Trondheim

1 Introduction

Research in fuel cells receives currently a lot of interest. Fuel cells can be used, in different layouts and types, to provide electric power to utilities as diverse as cars, laptop computers, mobile phones, or even to the electric grid as a power station. Research in all of these areas is extensive.

However, the dynamics of fuel cells has received comparatively less attention. Control of fuel cells, that requires having a dynamic model for numerical simulations, has received even less attention. A short overview of some papers published in the literature about dynamics and control of fuel cells follows.

1.1 Literature Review

Most dynamic models of fuel cells, such as for example in Amphlett et al. [1], normally consider current to be the system's input. While this is legitimate in a dynamic model, it must be remembered that current is not a directly manipulable input variable: it is rather the control objective than the means of control. Therefore, many models found in the literature will have to be adjusted to use manipulable inputs before they can be useful in a process-control setting. A proper means of control has to be clearly identified.

The model produced by Amphlett et al. [1] is essentially a thermal model with a basic, empirical modelling of the overvoltage effects. Cell current is considered a system input, and the catalytic overvoltage is assumed to vary instantly as a function of temperature, oxygen concentration and current. The model predicts well the behaviour of the stack in a time scale of minutes, but, since it does not treat the overvoltage as a state, it might be less accurate in the scale of seconds and lower.

One of the currently only two articles about fuel cells in the Journal of Process Control was written by Caux et al. [2]. They consider a system comprising a fuel cell, a compressor, valves, two DC/DC converters (a booster and a buck-boost converter). The analysis of the complete system is a step forward from the studies where the fuel cell had been seen as a separate entity from the rest of the process, but the fuel cell model itself is the same as from Amphlett et al. [1], and is therefore not treating overvoltage as a state; voltage variations will therefore be caused, directly, only by variations in temperature, current or oxygen concentration.

Golbert and Lewin [3] studied the application of model-predictive control (MPC) to fuel cells. They claimed that a sign inversion in the static gain between power output and current barred the possibility of using a fixed-gain controller with integral action, since it could not have been stabilised on such a process. They proceeded therefore to synthesise an MPC controller. Throughout the paper, Golbert and Lewin assume that current is a manipulable input, and use it to control the power output. Jay Benzinger pointed out[1], when the work was presented at the AIChE Annual Meeting of 2004, that it is not possible to use current (or voltage, which Golbert and Lewin's model also allows) as an input: he suggested the resistance of the external circuit as the variable one should rather use.

Two similar US patents have been granted to Lorenz et al. [4] and Mufford et al. [5], both concerning methods to control the power output of a fuel cell. Both these methods use air intake as the input variable. While this variable can indeed be set by manipulating the air-compressor speed, there are various reasons why this choice of input variable is not successful. First of all, only the fuel cells *per se* are considered: vital information is lost about the utility that will draw power from the cell. Also, while it could seem intuitive that a fuel cell will produce more power the more oxidant it is fed, this neglects a series of phenomena such as the mass-transport limit, the strong nonlinear effects of oxygen partial pressure in the cathode kinetics, the diffusion of oxygen through the cathode and the accumulation of oxygen in the cathode manifold.

Johansen [6] investigated, in his MSc thesis, the possibility of using reactant feed rate as an input in a control loop. He found that, when the feed rate was shut down, the fuel cell continued to produce power at an almost undisturbed rate, but dropped later, after about one minute. On the other hand, as soon as the reactant feed was reopened, the power output immediately reattained the previous values. This indicates that there is a dead time in which reactants in the manifolds must be consumed before the effect of reduced partial pressure can be apparent; the actual extent of this delay will depend, among others, on the sizing of the manifolds and on the rate of consumption of reactants. This effect, which is the same one encountered at the mass-transport limit when operating a fuel cell in normal conditions, is known to be nonlinear with reactant concentration, and its occurrence roughly corresponds with the depletion of one of the reactants. It must also be remarked that these effects are often not known precisely, as the cell's behaviour depends on many variables such as temperature, humidification, wear, and others.

Johansen's findings [6] indicate that the feed rate of reactants, in the specific case of the two patents [4, 5] oxygen, is a poor system input for a control layout. While it *can* be possible to control a fuel cell in such a way, the large delays and strong nonlinearities associated with the effect of the input on the system will eventually limit the system's performance in reference tracking and disturbance rejection.

In the PhD thesis by Pukrushpan [7] there is much about control of fuel cell systems, with focus on air-flow control and a large section about control and modelling of natural-gas fuel processors. Notwithstanding the high quality of the work, Pukrushpan has seemingly misquoted another author, Lino Guzzella [8], claiming that the time constants of electrochemical phenomena in fuel cells are in the order of magnitude of 10^{-19} seconds (Guzzella himself claimed 10^{-9} seconds). Pukrushpan did therefore not elaborate further on the electrochemical transient, whereas other authors have found that

[1] Comment made orally.

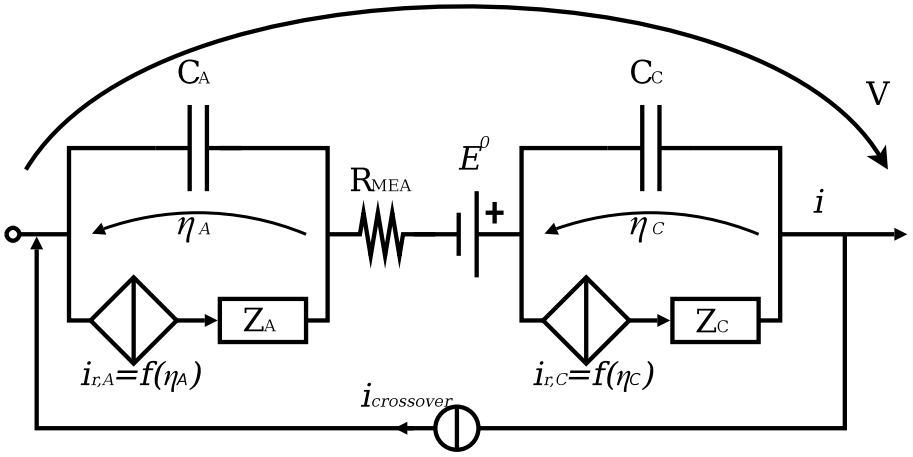

Figure 1: A detailed model of a fuel cell, with both electrodes modelled.

the time constants for the electrochemical transients are actually much higher [9, 10, 11, 12].

Ceraolo et al. [9] developed a dynamic model of a PEM fuel cell that included the dynamic development of the catalytic overvoltage. Whereas they did not apply their results to control, they produced a model that could easily be modified for control applications; they also included a model for multicomponent diffusion on the cathode side, based on Stefan-Maxwell equations.

Pathapati et al. [10] produced a model that calculated the overvoltage as in Amphlett et al. [1], integrating the catalytic overvoltage and non-steady-state gas flow analysis.

2 The Dynamic Model

Figure 1 shows how we can model a fuel cell to simulate its dynamic properties related to the electrochemical transient. This type of model is quite commonplace in electrochemistry; it consists of:

- a voltage generator, E^0;
- a resistance, R_{MEA};
- two electrodes, each with a capacitance (C_A and C_C) in parallel with a voltage-controlled current generator and an impedance;
- a current generator, $i_{crossover}$, that forces a certain current through the cell, even when this is in an open-circuit configuration.

The voltage generator E^0 represents the reversible potential: it depends on temperature and concentration of reactants at the reaction sites. The resistance in series with it represents the resistance to proton conduction in the membrane, and other resistances in series with it: its value depends mostly on temperature.

The capacitance of each electrode (C_A and C_C) represents a series of phenomena, often claimed to be the charge double layer [10]; however, these might also represent a number of other processes, as charged adsorbed species: in practice, these capacitances may lump together more than one phenomenon.

The voltage-controlled current generators ($i_{r,A}$ and $i_{r,C}$) in parallel with the capacitances are represented, in much of the electrochemical literature, by resistances. This can be misleading: these generators actually represent the Butler-Volmer equations, that depend exponentially, not linearly, on the overvoltage η, and can depend strongly on many other factors, as temperature, reactant concentration, presence of poisons as CO, etc.

The impedances Z_A and Z_C represent the *Warburg impedance*, that reflects the loss and lag occurring due to diffusion transients. These are usually important at high currents, where the reaction-site concentration of reactants is low, and is going to be a limiting factor. Some studies also claim that Gerischer impedance may be important for the anode [13].

The current generator, $i_{crossover}$, represents the crossover current, that lumps together a series of losses such as permeation of hydrogen or other reactants through the membrane, electronic conductivity of the membrane or similar ones. Its value is normally small, but has a significant effect: the overvoltage in a fuel cell (especially on the cathode) will increase rapidly with current at low values of current, and the presence of this small crossover current is what reduces the open-circuit voltage of the fuel cell from the theoretical value of the reversible potential.

2.1 Simplified model

The model presented in the previous section is more complex than what we need for our purposes. The anode, in particular, has a limited effect, and in most cases it can be neglected.

The Warburg impedance is also discarded, since it normally has its main effects close to the mass-transport limit, where the fuel cell should normally not operate. Also, a proper modelling of the Warburg impedance would require numerical solutions to multicomponent diffusion transients, which would heavily slow down the calculations.

The resulting model is shown in figure 2. The model has four parameters (E^0, R_{MEA}, C, and $i_{crossover}$) and a given function $i_r = f(\eta)$, that can contain a large number of parameters depending on the desired detail level. This simplification will be helpful in both numerical calculations and in theoretical understanding.

It must be kept in mind that the underlying hypothesis of this simplified model, i.e. neglecting the anodic overpotential, will be invalid if the hydrogen flow will be contaminated with poisons such as CO; in such a case, both electrodes will have to be modelled.

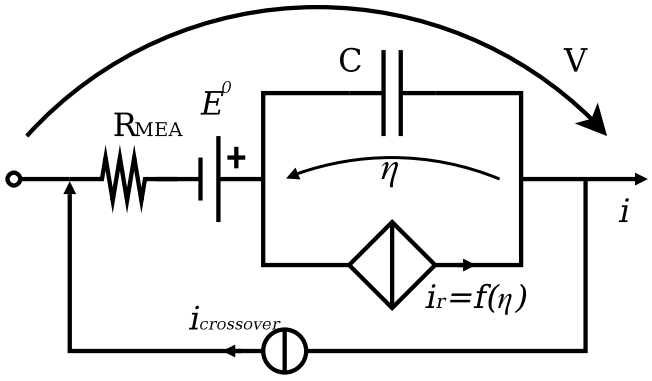

Figure 2: A simplified model of a fuel cell, with only one electrode.

3 Iso-η lines, or instantaneous characteristics

The plot of the relationship between current density i and voltage V in a fuel cell is widely known as a polarisation curve. Polarisation curves, however, represent this relationship at steady state, and do not give an indication about the way the fuel cell will behave during transients. To better understand this, we define the iso-η line, or *instantaneous characteristic*, to be the locus of all points that can be reached instantaneously by the fuel cell in the V-i plane.

Looking at figure 2, we see clearly that it contains a capacitor, and we know that the voltage across a capacitor is a state, according to the simple equation:

$$\frac{\mathrm{d}V}{\mathrm{d}t} = \frac{i}{C} \tag{1}$$

Therefore, the overvoltage η, which is the voltage over the capacitor, is a state of the fuel cell. The *reaction current* i_r, which represents the consumption of reactants, is a continuous, strictly increasing function of η, according to the Butler-Volmer equation (2), and is therefore another state.

$$i_r = i_0 \left(\mathrm{e}^{\alpha \frac{nF}{RT} \eta} - \mathrm{e}^{-(1-\alpha) \frac{nF}{RT} \eta} \right) \tag{2}$$

Since the Butler-Volmer equation (2) is bijective, i_r and η can be expressed as a function of each other (and of the other parameters in equation 2). However, the equation cannot be solved explicitly for η, and requires an iterative loop; this loop can be substantially accelerated using the Tafel approximation as an initial guess, as found in textbooks as Larminie and Dicks' [14].

Whereas the reaction current i_r varies continuously as a function of η and other variables, the current i exiting the fuel cell has no such requirement: the current through the capacitor is not a state, and can vary discontinuously. At steady state, η must be constant by definition, and the current through the capacitor must then be zero, which implies that $i + i_{crossover}$ be equal to i_r.

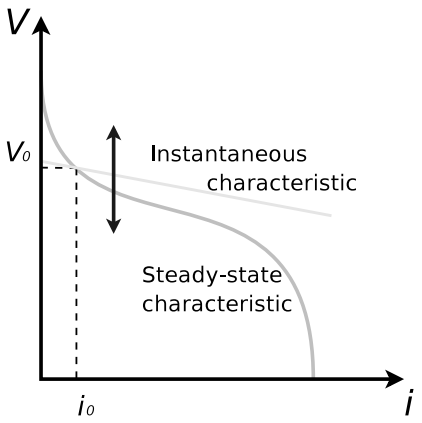

Figure 3: The steady-state polarisation curve and the instantaneous characteristic on a *V*-*i* plane. The instantaneous characteristic can move up or down according to the value of overvoltage η.

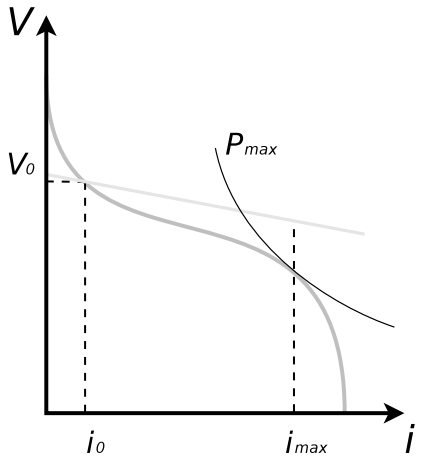

Figure 4: At current i_{max}, where the steady-state power output is maximum, the instantaneous characteristic from point (i_0,V_0) has a higher voltage than the polarisation curve.

When some variable (voltage, current, resistance of the external circuit) is changed discontinuously, or *stepped*, the overvoltage η will maintain a continuous variation, and not change value at the step time. Given that the reversible voltage E^0 will neither have a discontinuity at step time, only the voltage over the resistance term R_{MEA} is left to vary with current. This means that the instantaneous characteristic for a given operating point at reaction current i_r is:

$$V_{inst}(i_r, i) = E^0 - \eta(i_r) - R_{MEA}\, i \tag{3}$$

Since η varies continuously with time, the line of the instantaneous characteristic will rise or descend in the *V*-*i* plot, correspondingly to the value assumed by $\eta(i_r)$. If R_{MEA} is constant, the instantaneous characteristic will be a straight line, and it will cross the *V* axis at a voltage corresponding to $E^0 - \eta$.

We can now turn our attention to how specific transients develop. In general, the operating point will be at the intersection of the load's characteristic and the fuel cell's *instantaneous* characteristic. If the intersection point is not on the steady-state polarisation curve, the instantaneous characteristic will rise or sink, until the operating point will be brought to the intersection between the load characteristic and the polarisation curve. In general, the load might also be represented by an instantaneous characteristic, but for ease of treatment we will first consider stateless loads only.

In figure 5, a few simple transients have been sketched. They all start from a steady-state point on the polarisation curve, and illustrate the path of the operating point to reach the new intersection between the load. All transients are made of two parts:

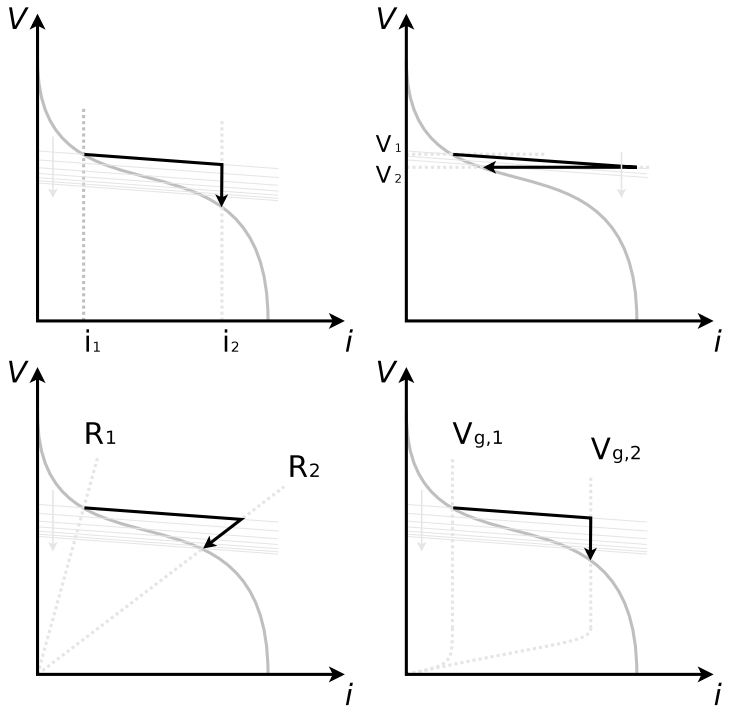

Figure 5: Some possible transient paths when stepping the outer circuit connected to a fuel cell. From top left and clockwise, a current step, a voltage step, a step in the gate voltage of a MOSFET and a resistance step.

1. After the step has taken place, the operating point *immediately* moves to the intersection of the current instantaneous characteristic and the new load.

2. Remaining on the external load's characteristic, the operating point follows the movement of the instantaneous characteristic, until it settles on the intersection between the external load and the polarisation curve.

It can already be remarked that the first part of the transient can result in significant power overshoots at step time, and this phenomenon will have significant consequences for control.

While the first two plots in figure 5 assume the presence of a current or voltage generator, and therefore an external power supply, the other two assume the presence of loads that can be changed with little or no external power supply. A resistance step may be done with a simple switch or using a rheostat, whereas a step in the gate voltage of a MOSFET[2] will require a voltage source: however, this source will have to provide a negligible amount of power. What is particularly interesting about rheostats or MOSFETs is that they can change their characteristic continuously with an input variable that can be directly manipulated.

[2]MOSFETs can be thought as valves that allow more current through them when their gate voltage is increased. For a detailed treatise of MOSFETs, see e.g. Mohan et al. [15].

4 Perfect Control of Fuel Cells

An important result can be obtained observing the instantaneous characteristics in the previous figures. We see clearly that they pass by the current corresponding to the maximum power output with an higher voltage than the polarisation curve. It is an immediate observation that this means that we can, at least in theory, step the power output of the fuel cell even beyond the maximum nominal value. We shall now seek to properly formalise this finding.

We shall define i_{max} and P_{max} to be the current and the power output at the point, on the steady-state polarisation curve, where the power output from the cell is maximum.

Theorem 4.1 (Perfect control of fuel cells) *Given a fuel cell with steady-state*[3] *voltage expressed by* $V_{ss}(i) = E^0 - \eta(i_r) - R_{MEA}(i)\, i$*, with overvoltage* $\eta(i_r)$ *strictly increasing with* i_r*, and internal resistance* $R_{MEA}(i)$ *continuous in* i*, it is always possible to instantaneously step the power output to any value between zero and its maximum steady-state value from any operating point, both transient and steady-state, lying on an instantaneous characteristic intersecting the polarisation curve at some* $i \in [0, i_{max}]$.

Proof Given any fixed $i_0 \in [0, i_{max}]$, we can identify the corresponding instantaneous characteristic $V_i(i) = E^0 - \eta(i_0 + i_{crossover}) - R_{MEA}(i)\, i$. Since $\eta(i_r)$ is strictly increasing with i_r, $\eta(i_{max} + i_{crossover}) \geq \eta(i_0 + i_{crossover})$.

It follows that $V_i(i_{max}) - V_{ss}(i_{max}) = -\eta(i_0 + i_{crossover}) + \eta(i_{max} + i_{crossover}) \geq 0$, that means that at current i_{max} the instantaneous characteristic will have a higher voltage than the steady-state one, and thereby a larger power output: $P_i(i_{max}) \triangleq V_i(i_{max})\, i_{max} \geq V_{ss}(i_{max})\, i_{max} \triangleq P_{ss}(i_{max})$.

Power along the instantaneous characteristic varies continuously, according to the formula $P_i(i) = V_i(i)\, i$, because $R_{MEA}(i)$ is continuous. It is trivial that power output can be set to zero by setting $i = 0$. For the intermediate-value (Darboux) property, $\exists\, i : P_i(i) = P, \forall P \in [0, P_{max}]$. □

This theorem guarantees, therefore, that there is a way to change instantaneously to any value of power output in the complete power range of the fuel cell, from zero to maximum, under very general conditions. This means there is no inherent limitation to how fast control we can achieve, even though practical issues such as measurement time and computation time will eventually pose a limit.

This has also other implications: if incorrectly controlled, a fuel cell might exhibit large spikes in power output, which may damage equipment connected to it. This might be especially important in microelectronics appliances.

[3] Remember that at steady state $i_r \triangleq i + i_{crossover}$.

4.1 Implicit Limitations

Theorem 4.1 delivers an important result, but makes some implicit assumptions. The assumption about the form of the function describing the polarisation curve is especially important, since the curve is expected to be only a function of the circuit and reaction currents: other factors such as temperature, catalyst poisoning, reactant concentration are left out. Therefore, *the theorem is valid only in the context of a certain set of states*: we are only guaranteed that we can instantly reach the maximum power output for those conditions of temperature, composition, etc., which may be less than the nominal power output that the fuel cell is supposed to deliver in design conditions. In such a case, other control variables may be used to modify these states, and might pose some performance limits; for instance, a temperature increase in the cell cannot occur stepwise.

5 Fuel Cells and DC/DC Converters

A DC/DC converter can connect a fuel-cell stack and an appliance, converting the power from the fuel cell in an appropriate form. According to Luo and Ye [16], there are over 500 different topologies of converters. The most simple are the *boost* converter, that increases voltage from input to output, and the *buck* converter, that decreases it; other types are the *buck-boost* and the *Ćuk* converters.

The buck-boost converter is chosen for this paper. The reasons are that it can convert power in a wide range of voltages, both above and below the cell stack's. The buck or the boost converters alone, instead, could only respectively reduce or increase the input voltage.

In a real application, a more complex, four-quadrant converter would probably be preferred. Such a converter would be able to deliver power from the fuel cell to the motor, and to implement regenerative braking by transferring power from the motor to a battery or a capacitor; it would also be able to invert the sign of voltage, to drive and brake the vehicle in reverse. In this study, only the case of a first-quadrant converter will be considered, for sake of simplicity.

5.1 Fuel Cells coupled with Converters

In buck-boost converters, we usually have a discontinuous current passing through the input, in our case a fuel cell stack. Since the switching frequency will in most cases be much faster than the transients in the cells, it is common to work with averaged units [17].

Of particular interest is the case of a current stepping between a certain value and zero at regular intervals. Defining D to be the fraction of time, also known as the *duty ratio*, during which a current I passes through the cell, we immediately find that the reaction current (the one corresponding to the consumption of reactants) is $I_r = I\,D$ when averaged over a sufficiently long time[4]. If the

[4]Here we are neglecting the effect of the crossover current.

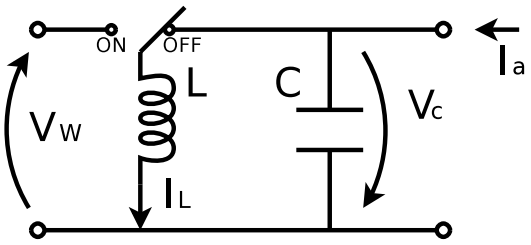

Figure 6: A basic representation of a buck-boost converter; V_W is the input voltage.

switching frequency is substantially faster than the electrochemical dynamics, we may assume the overvoltage to be constant: $\eta \approx \eta(i\,D)$. However, the cell voltage loss caused by the linear resistance has no transient associated, and will depend directly on the current, no matter it is applied only a fraction of the time. Therefore, calling V_W, or *working voltage*, the voltage obtained by a fuel cell under a rapidly switching current that has value I for a fraction D of the time, we obtain:

$$V_W = E - \eta(i\,D) - R\,I \tag{4}$$

This voltage is the actual input voltage that the DC/DC converter will work with.

5.2 Buck-Boost Converters

A buck-boost converter is sketched in figure 6. The voltage source is connected in parallel, through a switch, to an inductor. When the switch is on, the inductor accumulates power by storing energy in its magnetic field.

The inductor current varies continuously, as it is a state. When the switch is off, the current is therefore forced into the capacitor that the inductor is now in parallel with, moving the energy stored in the inductor's magnetic field into the capacitor's electric field.

Independently from the switch's state, the capacitor is continuously exchanging power with an external load.

In this layout, we assume that the cell stack's voltage V_W and the external load's current I_a are measurable at all times.

Since we know from theorem 4.1 that fuel cells can immediately deliver their maximum power, the DC/DC converter parameters will be the main limit to our performance. Lower values for the capacitance and the inductance will increase the transient's speed and accelerate the overall response, but will require faster switching. In this paper we will use the values previously used in a boost converter designed in Caux el al. [2], namely $L = 0.94\,\text{mH}$ and $C = 3.2\,\text{mF}$.

The equations describing this system are, when the fuel-cell stack is connected to the inductor:

$$L \frac{\mathrm{d}I_L}{\mathrm{d}t} = V_W \tag{5}$$

$$C \frac{\mathrm{d}V_C}{\mathrm{d}t} = -I_a \tag{6}$$

V_W and I_a are considered to be external entities with respect to the DC/DC converter, and are assumed to maintain a positive sign. The trajectories described by these equations are clearly straight lines[5].

When the switch is positioned in such a way that the inductor is connected to the capacitor, the equations are instead:

$$L \frac{\mathrm{d}I_L}{\mathrm{d}t} = -V_C \tag{7}$$

$$C \frac{\mathrm{d}V_C}{\mathrm{d}t} = I_L - I_a \tag{8}$$

The trajectories described by these equations are a series of ellipses, centred at the point $(0,\ I_a)$, whose parametric equation can be given as:

$$\frac{1}{2}L\,(I_L - I_a)^2 + \frac{1}{2}C\,V_C^2 = k \qquad k \in \mathbb{R}_0^+ \tag{9}$$

It would be tempting to define these curves as representatives of the amount of energy physically stored in the converter, but the first term in equation 9 is not the energy stored in the inductor's magnetic field. The value of k, however, can indeed be mathematically interpreted as representative of the system's energy.

The trajectories corresponding to these equations are shown in figure 7.

5.3 Sliding-Mode Control

Sliding-mode control is a common technique for control of DC/DC converters. In this technique, a switch (often an IGBT or a MOSFET) or a series of switches are set to an open or closed state depending on some logic rule.

[5] In reality, V_W depends on I_L, as $V_W = E - \eta - R\,I_L$. However, such an assumption would require a cell-specific parameter, R, to be provided. It will be assumed that R is small enough to justify an assumption of positive V_W in the area of interest.

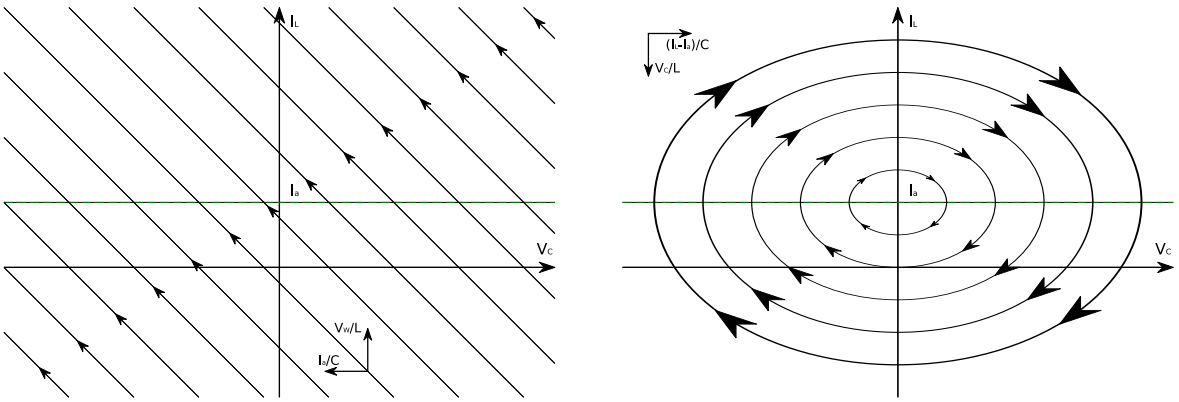

Figure 7: The trajectories of the state variables in a buck-boost converter in the V_C-I_L plane. On the left-hand side, energy is collected from the input by the inductor. On the right-hand side, no energy is drawn from the source, and the energy stored in the inductor is exchanged with the capacitor. The capacitor delivers power to the output in both configurations. In a real system, the trajectories in the right-hand sides would be spirals, because of losses in the switches.

These rules are designed to maintain the operating point of the system on a so-called *sliding surface*, usually by defining the state of the switches as a function of the position of the operating point relatively to the sliding surface; the *existence condition* for a sliding mode is that, given these rules, the operating point will always move towards the sliding surface, and on it "slide" towards the desired set point. A more detailed explanation, with examples, has been written by Spiazzi and Mattavelli [18].

5.4 Control Rules

Control of the DC/DC converter will be understood having the following objective: *to control the output voltage V_C so that it is close to reference V_{ref}, in spite of external disturbances I_a and V_W, by manipulating the switch in the buck-boost controller*. In other words, we will try to maintain a certain value of V_C by properly switching the system between its two substructures (as shown in figures 6 and 7).

The control algorithm will consist of a series of *switching rules*. This is strictly speaking not sliding-mode control, as no one of the defined surfaces is actually a sliding mode. The rules, however, make sure that the target point with voltage V_{ref} is reached.

Energy level If the value of k in equation 9 is not sufficiently high, the elliptical trajectories of the OFF mode will not be able to reach V_{ref}. Therefore, the only possibility left is to switch to the linear trajectories of the ON mode until a sufficiently high energy level is reached.

The *sufficiently high* energy level is however not the one corresponding to an ellipse that has its extreme point in V_{ref}. If it were so, it would not be possible to maintain the operating point at that value by switching to the ON mode: the ON mode, which in general has a non-zero component along the V_C axis, would cause the system to reach a lower energy level, at which

it should maintain the ON state until reaching again a high enough energy level. An hysteresis cycle would then result, which would be an unsatisfactory performance.

The correct energy level is then the one corresponding to the ellipse that, at the reference voltage V_{ref}, is *tangent* to the lines of the ON mode. The unavoidable imprecision in parameter estimation and measurement will cause some oscillation, however.

The mathematical description of the rule is:

$$\frac{1}{2} C V_C^2 + \frac{1}{2} L (I_L - I_a)^2 < \frac{1}{2} C V_{ref}^2 + \frac{1}{2} L \left(\frac{V_{ref} I_a}{V_W} \right)^2 \Rightarrow \mathsf{ON} \tag{10}$$

High-voltage switch At voltages higher that V_{ref}, the surface at which one moves from one substructure to the other is given by the tangent line departing from the ellipse described above, at voltage V_{ref}. Since this line is by construction parallel to the lines of the ON mode, once the operating points, moving along the OFF-mode ellipses, crosses this line, it is not possible for it to return back. This is important because there is no guarantee that the component of the ON-mode derivatives along a given line are larger than the OFF-mode's, because the former are disturbances that we do not directly control.

The mathematical description of the rule is:

$$V_C > V_{ref} \quad \wedge \quad I_L - I_a < \frac{V_{ref} I_a}{V_W} - \frac{C}{L} \frac{V_W}{I_a} \left(V_C - V_{ref} \right) \Rightarrow \mathsf{ON} \tag{11}$$

Low-voltage switch It is not unlikely that, during transients, voltage V_C will reach negative values. In fact, it is quite a common phenomenon, albeit lasting only for a short time. A reasonable control objective is to minimise the inverse response during such a transient. Therefore, if during a transient V_C is less than zero, and the energy level is sufficient as defined above, the switch from ON mode to OFF mode should be at the point where the ON lines are tangent to an ellipse, which is the lowest-energy point they will reach.

The mathematical description of the rule is:

$$V_C < 0 \quad \wedge \quad I_L - I_a < \frac{V_C I_a}{V_W} \Rightarrow \mathsf{ON} \tag{12}$$

An additional rule may be easily implemented if we desired to avoid negative values of current I_L, but the short duration of transients should not pose a threat of reverse electrolysis[6]. However, if that were the case, one could simply implement:

$$I_L < 0 \Rightarrow \mathsf{ON} \tag{13}$$

The rules are graphically plotted in figure 8. It is understood that if no one of rules matches, the default state will be OFF.

[6] Of course this is relevant only for the ON mode, when current is actually passing through the fuel-cell stack.

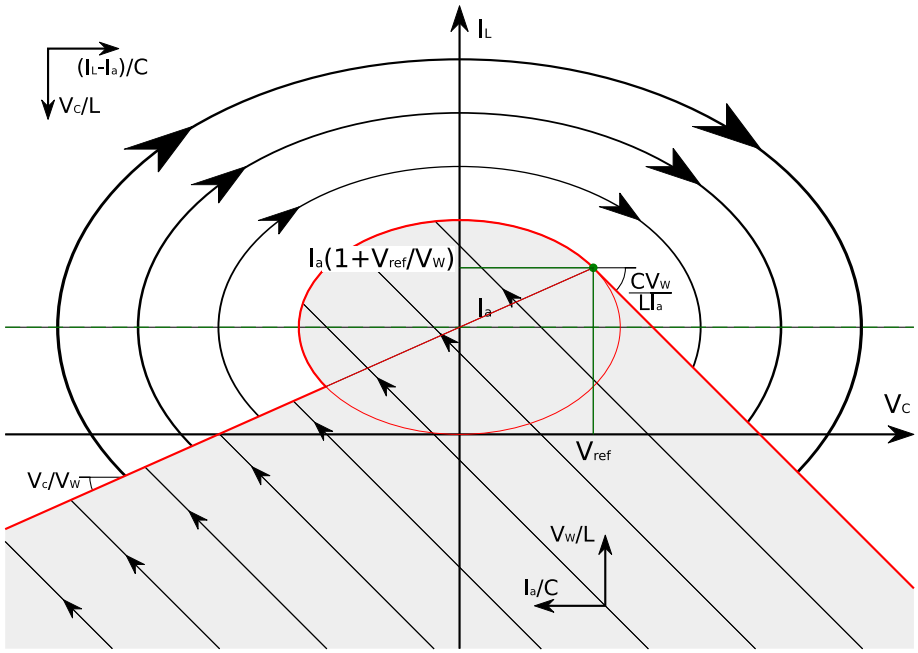

Figure 8: Graphical representation of the switching rules to control a DC/DC buck-boost controller. Remark that the inclination of the ON lines (in the greyed-out area), the inclination of the switching lines at high and low voltage, and the size and vertical positioning of the central elliptical part all depend on the values of the reference voltage and the disturbances.

5.5 Control Performance

Some preliminary conclusions can be drawn by looking carefully at figure 8.

- Steps in V_{ref} will in general exhibit an inverse response. When increasing, the operating point will have to accumulate energy along the ON-mode lines, which will cause an initial reduction of V_C. When decreasing, the operating point will follow the OFF-mode lines until it will reach either their maximum value of voltage, or the switching surface described by rule 11, before decreasing again.
- Steps in I_a will have a similar effect, but this is intuitive: more current at the output, at the same output voltage, means more power delivered, and the converter will have to gradually adapt to this new regime.
- The set of rules does not permit to specify a negative V_{ref}. This is intentional, because, with a positive I_a, power would be drawn from the outer circuit to the fuel cell, causing reverse electrolysis, and likely damaging the fuel cell's catalyst.

A simulated transient is shown in figure 9. It can be noticed how the inverse response is much more significant at high values of I_a. The transients have typically quick settling times, about 5 ms: this is faster than the required 0.02 s (according to Soroush [19]).

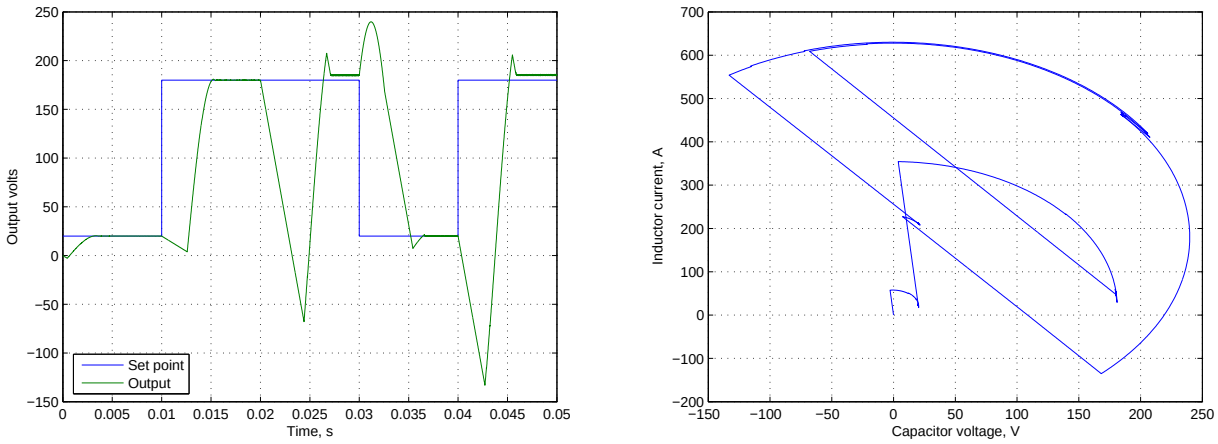

Figure 9: Simulated transient of a DC/DC buck-boost converter, controlled with switching rules. The external current is initially 20 A, and is stepped to 180 A after 0.02 s. The switching frequency has been set to 10 μs. On the right, a phase-plane plot is presented.

6 Application to a DC Electric Motor

It has been shown in figure 5 that the shape of the characteristic of the external load has a strong effect on how the transient develops in the fuel cell. It is therefore generally desirable, when designing a controller for a fuel cell, to consider a description of the load as well. In other words, the controller is not for the fuel cell alone, but for the whole system. In this section, an electric motor for a fuel-cell powered car will be considered; for simplicity, a regenerative braking system is not going to be modelled.

6.1 Electric DC motors

Dual-current motors have for a long time been the only type of electric motor that could be easily controlled. The reason of this preference is due to the simplicity of controlling the main variable in DC motors, the input current, as opposed to the difficulty of controlling the input frequency in alternated-current motors.

Whereas microelectronics has made it practical to control AC motors too, this paper will consider a DC motor as the load to which the fuel cell is connected. So-called “brushless DC motors” are in actuality AC motors with a electronic interface that makes them appear like DC ones to the outside circuit, with the benefit of disposing of the brushes, which are often the main limit to the motor’s lifetime.

Generally speaking, there are two main variables influencing the power output in a DC motor’s mathematical model (figure 10): the armature current and the field-winding current. The armature current, I_a, is directly proportional to the torque exerted by the motor, divided by the magnetic field Φ_e.

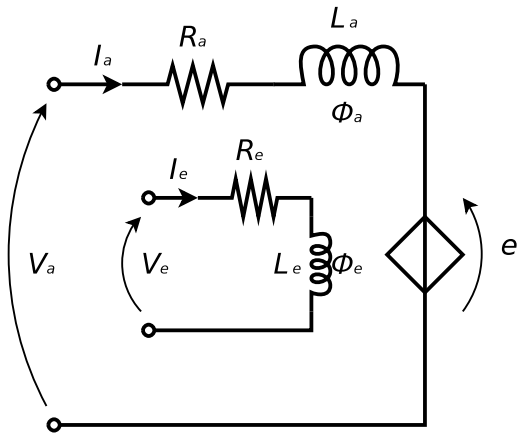

Figure 10: A typical model of a DC motor [20].

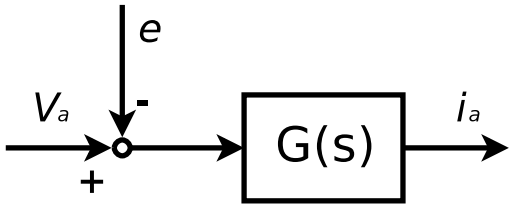

Figure 11: The process flow diagram of a simple DC motor with constant magnetic flow; the transfer function is $G(s) = \frac{1}{L_a\, s + R_a}$.

The voltage generator e in figure 10 represents the counter-electromotive force induced by the rotation of the shaft. Its value is directly proportional to the angular velocity multiplied by the magnetic flux Φ_e.

The field-winding current, which usually absorbs just a small fraction of the total power consumption, generates the magnetic field in which the armature current passes; by weakening the field, it is possible to increase velocity at the expense of torque, by modifying the proportionality ratio between armature current and torque [20]. However, for vehicle applications, higher velocity usually means higher torque too, because of wind resistance: in this paper, therefore, a permanent-magnet motor will be considered, or, equivalently, a motor with constant field winding current.

Such a simplified model can be described by the following equations:

$$V_a = R_a\, I_a + L_a \frac{\mathrm{d}I_a}{\mathrm{d}t} + e \tag{14}$$

$$e = k\, v \tag{15}$$

$$I_a = \frac{F}{k} \tag{16}$$

6.1.1 Value of k

Constant k is the same in equations 15 and 16, since the electric power input must be equal to the mechanical power output ($F\, v = e\, I_a$). Constant k includes the rotation radius as well, so that we may work in terms of force F applied by the motor to the vehicle and the vehicle's velocity v instead of the motor's torque T and angular velocity ω. In practice, constant k can be set with a gearbox [21].

Larminie and Lowry [21] claim that a common parameter for electric-vehicle motors is a maximum nominal armature current of 250 A. Considering that standard driving cycles, such as the New European Driving Cycle, result in a maximum force requirement of about 1250 N when applied on a average-sized car, we can use equation 16 to obtain a reasonable value for k:

$$k = \frac{F}{I_a} \approx 5\,\mathrm{N/A} \tag{17}$$

6.1.2 Control Variables

Rearranging equation 14, we can more easily see that I_a is a state[7] of the motor.

$$L_a \frac{\mathrm{d}I_a}{\mathrm{d}t} = V_a - R_a\, I_a - e \tag{18}$$

From here, it is easy to transpose this equation in the Laplace domain:

$$I_a = \frac{1}{L_a\, s + R_a}\,(V_a - e) \tag{19}$$

Larminie and Lowry [21] present the typical values of 0.02 mH for L_a and 0.02 Ω for R_a.

A graphical representation of this system is presented in figure 11. We see clearly that I_a is the output and $V_a - e$ is the input.

Since e is a direct consequence of vehicle motion, it is not possible to modify it without acting on the vehicle speed; this would be undesirable, because the driver will control manually the velocity by acting on the accelerator pedal (and therefore I_a). The counter-electromotive force e will therefore be interpreted as a *disturbance*.

It is however possible to compensate for this disturbance by manipulating the input voltage V_a. The control problem is therefore to control I_a by manipulating V_a, in spite of disturbance e.

We can set voltage V_a by connecting the motor input to a buck-boost converter's output. The control performance that was indicated in the section on DC/DC converter control can be now interpreted as *actuator dynamics*. This is an example of *cascade control*: control of I_a is obtained by controlling V_C, which is in turn obtained by switching between the buck-boost converter's ON and OFF modes.

6.2 Approximation of a buck-boost converter

In order to obtain a controller, it can be useful to approximate the actuator dynamics as a transfer function. Looking at figure 9, we can assume that the actuator dynamics can be approximated by the following transfer function:

[7] *State* means here a variable that is a differential state in an ordinary differential equation.

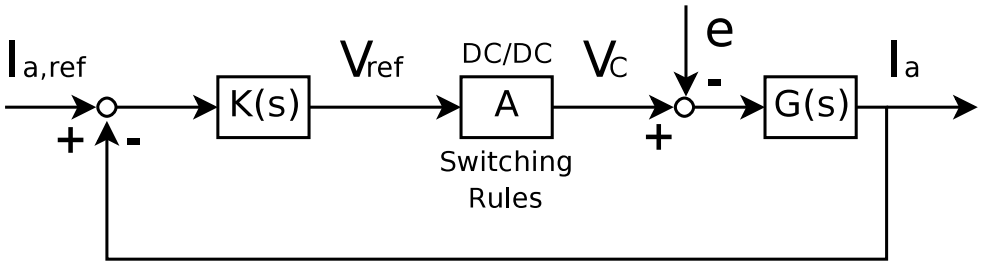

Figure 12: The cascade control structure of the proposed layout.

$$A(s) = \frac{\mathrm{e}^{-\theta s}}{\tau s + 1} \tag{20}$$

Where both the delay θ and the time constant τ are estimated at about 5 ms. The delay θ is assumed to be an *effective* delay, actually representing the inverse response; Skogestad [22] claims that "*an inverse response has a deteriorating effect on control similar to that of a time delay*".

6.3 PI Controller Synthesis

Having a complete, however approximate description of the system, we can proceed to synthesise a PI controller according to the SIMC rules [22]. The resulting controller is:

$$K(s) = K_c \left(1 + \frac{1}{\tau_I\, s}\right) \tag{21}$$

Where we select $K_c = 2$ and $\tau_I = 40$ ms.

It is now possible to make simulation runs of the whole control system. A brief series of transients is simulated in figure 13. It is assumed a vehicle is moving at 40 km/h[8], and that a series of steps in the armature current's reference[9] are performed.

The resulting control performance seems to be satisfactory, with rise times of at most 50 ms in all transients; some overshoot is observed, but the transient is settled in all cases after 0.2 s.

[8]The speed is kept constant in the simulation, for simplicity and to make the results comparable.

[9]Steps in the armature current are proportional to steps in torque output.

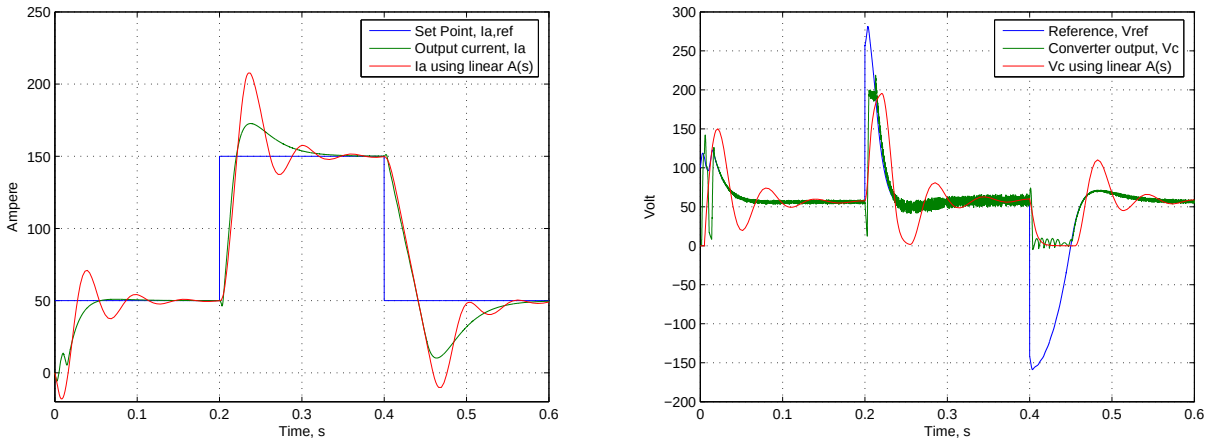

Figure 13: Simulation of a series of steps in reference for the system in figure 12. On the left, the set point $I_{a,ref}$ and value of the armature current in the electric motor I_a. On the right, the PI controller's output V_{ref} is the reference signal for the DC/DC converter. The switching frequency in the DC/DC converter is $100\,\mu$s. In both plots, the results obtained using the linear approximation for the converter presented in equation 20, instead of the complete nonlinear model, are also shown. The output of the controller has been limited to $V_{ref} \in [0, 200]\,\mathrm{V}$.

7 Conclusion

This article has first analysed from a theoretical point of view the electrochemical transient of fuel cells, introducing the concept of instantaneous characteristic of a fuel cell and how it influences the shape of transients in the voltage-current density phase plane.

These results have been used to demonstrate that it is always possible to instantaneously step the power output of a fuel cell to its maximum (meant as the maximum at the present temperature, partial pressures, catalyst poisoning etc.) under broad conditions.

A method to control the output voltage of a buck-boost converter connected to a fuel cell was presented. The method is based on switching the converter based on a few simple logical rules. The resulting performance has been deemed satisfactory, with transients settling after about 5 ms.

The resulting control loop has then been inserted in a cascade-control framework (figure 12) to control the armature current in a DC motor by manipulating its input voltage. The results have been in excess of specifications given elsewhere in the literature [19], with rise times of about 50 milliseconds and settling times of less than 0.02 seconds (figure 13).

The PI controller, when applied with approximated actuator dynamics, gave satisfactory results in reference tracking and disturbance rejection.

Acknowledgements

This work has received financial support from the Norwegian Research Council and Statoil AS.

References

[1] J. C. Amphlett, R. F. Mann, B. A. Peppley, P. R. Roberge, A. Rodrigues, A model predicting transient responses of proton exchange membrane fuel cells, Journal of Power Sources 61 (1996) 183–188.

[2] S. Caux, J. Lachaize, M. Fadel, P. Shott, L. Nicod, Modelling and control of a fuel cell system and storage elements in transport applications, Journal of Process Control 15 (2005) 481–491.

[3] J. Golbert, D. R. Lewin, Model-based control of fuel cells: (1) regulatory control, Journal of Power Sources 135 (2004) 135–151.

[4] H. Lorenz, K.-E. Noreikat, T. Klaiber, W. Fleck, J. Sonntag, G. Hornburg, A. Gaulhofer, Method and device for vehicle fuel cell dynamic power control, US patent 5 646 852, assigned to Daimler-Benz Aktiengesellschaft (July 1997).

[5] W. E. Mufford, D. G. Strasky, Power control system for a fuel cell powered vehicle, US patent 5 771 476, assigned to DBB Fuel Cell Engines Gmbh (June 1998).

[6] R. L. Johansen, Fuel cells in vehicles, Master's thesis, Norwegian University of Science and Technology (2003).

[7] J. T. Pukrushpan, Modeling and control of fuel cell systems and fuel processors, Ph.D. thesis, Department of Mechanical Engineering, University of Michigan, Ann Arbor, Michigan, USA (2003).

[8] L. Guzzella, Control oriented modelling of fuel-cell based vehicles, in: Nsf workshop on the integration of modeling and control for automotive systems, 1999.

[9] M. Ceraolo, C. Miulli, A. Pozio, Modelling static and dynamic behaviour of proton exchange membrane fuel cells on the basis of electro-chemical description, Journal of Power Sources 113 (2003) 131–144.

[10] P. R. Pathapati, X. Xue, J. Tang, A new dynamic model for predicting transient phenomena in a pem fuel cell system, Renewable energy 30 (2005) 1–22.

[11] H. Weydahl, S. Møller-Holst, G. Hagen, Transient response of a proton exchange membrane fuel cell, in: Joint International Meeting of The Electrochemical Society, 2004.

[12] F. Zenith, F. Seland, B. Børresen, R. Tunold, S. Skogestad, Experimental study and control-oriented simulation of the transient response of a high-temperature polymer fuel cell, Journal of Power Sources(Submitted).

[13] A.-K. Meland, D. Bedeaux, S. Kjelstrup, A Gerischer phase element in the impedance diagram of the polymer membrane fuel cell anode(Submitted).

[14] J. Larminie, A. Dicks, Fuel Cell Systems Explained, 1st Edition, Wiley, 1999.

[15] N. Mohan, T. M. Undeland, W. P. Robbins, Power Electronics: Converters, Applications and Design, 2nd Edition, John Wiley & Sons, Inc., 1995.

[16] F. L. Luo, H. Ye, Advanced DC/DC Converters, crc press, Boca Raton, Florida, USA, 2004.

[17] J. P. Agrawal, Power Electronic Systems — Theory and Design, Prentice Hall, 2001.

[18] G. Spiazzi, P. Mattavelli, The Power Electronics Handbook, Industrial electronics, CRC press, 2001, Ch. 8.

[19] M. Soroush, Y. A. Elabd, Process systems engineering challenges in fuel cell technology for automobiles, in: AIChE Annual Meeting, 2004.

[20] W. Leonhard, Control of Electrical Drives, 2nd Edition, Springer, 2001.

[21] J. Larminie, J. Lowry, Electric Vehicle Technology Explained, Wiley, 2003.

[22] S. Skogestad, Simple analytic rules for model reduction and pid controller tuning, Journal of process control 13 (2003) 291–309.